Journal of Engg. Research, Special Issue, October 2019 pp. 63-75

Stearic Acid-Modified CuO Coating Metal Surface with Superhydrophobicity and Anti-Corrosion Properties

Satria Robi Trisnanto*, Iwan Setiawan*, Gagus Ketut Sunnardianto** and Farid Triawan*

**Faculty of Engineering and Technology, Sampoerna University, Jakarta, 12780, Indonesia*
***Research Center for Chemistry, Indonesian Institute of Sciences (LIPI), Tangerang Selatan, 15314, Indonesia*
**Corresponding Author: iwan.setiawan@sampoernauniversity.ac.id*

ABSTRACT

A flower-like superhydrophobic CuO coating had been successfully fabricated on low-carbon steel surfaces. The surfaces were prepared by electrodeposition of Cu combined with solution immersion in a mixture of NaOH and H_2O_2 solution, as well as stearic acid modification. According to the contact angle measurements, the superhydrophobic CuO coating demonstrated a maximum contact angle of 171.4 ± 1.56° with a minimum sliding angle of 7.2 ± 0.43°. Therefore, it could be considered as possessing superhydrophobic property. The superhydrophobic property was achieved by surface roughening and stearic acid deposition as the low-surface-energy modifier. Furthermore, the corrosion test using weight loss technique was performed to quantify the anti-corrosion property. It was found that the superhydrophobic CuO coating had a corrosion inhibition efficiency of more than 70%.

Keywords: Copper oxide; corrosion protection; low-carbon steel; superhydrophobic coating; stearic acid.

INTRODUCTION

Ferrous metals such as steel are one of the most used metals to produce various modern industrial products. This is because the cost of steel is relatively cheaper in comparison with other metals. Because of the economic benefits, steel is commonly used in construction and transportation systems (Li *et al.*, 2016). However, despite the strength, steel is vulnerable to environmental effects such as high acidity, temperature changes, and high humidity conditions. It is found that many steel failures are mainly due to those environmental effects, which lead to corrosion. Because of the corrosion, 20% of global energy has lost along with material lost caused by steel degradation (Vazirinasab *et al.*, 2018).

Current techniques in corrosion prevention are complex and non-environmentally friendly, such as cathodic protection and corrosion inhibition (Whelan *et al.*, 2004). Cathodic protection is considered as a complex method in corrosion protection strategy. Its implementation is limited to immerse structure only. Therefore, it is not applicable to prevent atmospheric corrosion. Other techniques such as corrosion inhibition involve hazardous chemical decanethiol (Whelan *et al.*, 2004) and according to Materials Safety Data Sheet (MSDS), decanethiol is considered as toxic chemical category 4. Regarding those issues, a passive method such as protective coating seems to be used as a potential for corrosion protection.

Recently, the superhydrophobic surface has attracted wide attention from scientists and engineers. This interest is driven by potential application of superhydrophobic coating for anti-fouling (Li *et al.*, 2016), self-cleaning (Hao *et al.*, 2016), anti-icing (Subramanyam *et al.*, 2016), oil-water separation (Kong *et al.*, 2015), and anti-corrosion (Brassard *et*

al., 2015). Inspired by lotus' hydrophobicity property, artificial superhydrophobic on various materials can be achieved by modifying the surface morphology and energy. In order to imitate the lotus hydrophobicity property, many researchers are trying to find the most appropriate way to fabricate a superhydrophobic coating on the metal substrate.

Previous studies reported that metal surfaces could be modified using various techniques to prevent corrosion (Asmara and Kurniawan, 2018; Kurniawan *et al.*, 2016). The reported methods include electrodeposition (Hao *et al.*, 2015; Hao *et al.*, 2016), spray coating (Zhang *et al.*, 2014), dip and spin coating (Ganapathy *et al.*, 2018), and plasma treatment (Triawan *et al.*, 2018). Furthermore, the superhydrophobic coating had also been fabricated using a fluorine-based modifier to lower the surface energy. A biomimetic superhydrophobic ZnO coating on X90 steel had been successfully generated from perfluorooctanoic acid using a specific method reported in the literature (Hao *et al.*, 2015). A robust superhydrophobic surface was achieved by fluorinated silane treatment on aluminum foil (Zhang *et al.*, 2015). In addition, a superamphiphobic copper surface with multilevel structures had been fabricated through oxidation, displacement reaction, and fluorinated treatment using 1H,1H,2H,2H-perfluorodecanethiol (Wen *et al.*, 2018). However, despite having great potential to create superhydrophobic and superamphiphobic coatings, fluorinated modifiers are considered hazardous material.

Recently, studies to find a non-toxic surface modifier are gaining more interest. Stearic acid is one of the alternative materials due to its non-toxicity property and relatively lower cost in comparison to other modifiers. Therefore, it has a high potential to be used as a chemical modifier. Stearic Acid has been used in preparing, e.g., a superhydrophobic ZnO coating on a glass substrate (Gurav *et al.*, 2014; Zhang *et al.*, 2016) and a superhydrophobic zinc nano-coating in X65 steel substrate (Feng *et al.*, 2018).

In this work, the possibility of implementing stearic acid on a CuO-coated steel substrate as a surface modifier in order to fabricate a superhydrophobic coating using a series of facile methods was explored. A superhydrophobic CuO coating on steel substrate was prepared through a series of treatments, which include electrodeposition, solution-immersion, and stearic acid modification. Surface characterization by Scanning Electron Microscope (SEM) and Energy Dispersive X-Ray Spectroscopy (EDS), corrosion test, and wettability test were carried out. As a result, the fabricated superhydrophobic CuO coating surface exhibited excellent water-repellency as well as anti-corrosion properties.

METHODS

Specimen preparation

The low-carbon steel plates with the chemical composition of 99.27% of Fe, 0.11% of C, 0.24% of Si, 0.35% of Mn, 0.017% of P, and 0.013% of S obtained from a local store (Santo Jaya Teknik) were cut into the size of 50 x 20 x 2 mm. A copper plate with high purity (> 97.5%) was used as an anode. All materials and chemicals include NaOH, Na_2CO_3, Na_2SiO_3, $CuSO_4$, anhydrous ethanol, H_2O_2, and stearic acid of analytical grade and were used without further purification.

The specimens were polished using silicon carbide (SiC) abrasive paper ranging from 180 to 1200 grit to remove the pre-coated surface and smoothen the surface. Finally, the specimens were rinsed with distilled water and anhydrous ethanol to dissolve remaining contaminants and then the specimens were dried. The alkali cleaning process was performed after the specimens had been polished. The alkali cleaning process was done to remove grease from the substrate surface. Degreasing treatment was done by immersing steel specimen into a solution containing 30 g/L of NaOH, 20 g/L of Na_2CO_3, and 10 g/L of Na_2SiO_3 at 60°C (Hao *et al.*, 2016; Li and Yu, 2016; Li and Yu, 2017). Finally, the substrates were removed after 15 minutes of immersion and rinsed with distilled water.

The fabrication of superhydrophobic CuO coating was performed with the following steps as also illustrated in Figure 1:

- Electrodeposition of Cu on steel. Electrodeposition is a facile method, which consists of a voltage source, electrolyte, and electrode (cathode and anode). A clean steel substrate was used as a cathode and copper plate was used as an anode. The Cu electrodeposition had been conducted at various deposition times and electrolyte concentrations. The optimum parameters were determined from static contact angle measurement (Trisnanto *et al.*, 2018).
- Solution-immersion in H_2O_2. In this experiment, the CuO layer was fabricated by the solution-immersion method. It is a simple, facile, and inexpensive method to grow CuO crystal layer. It was done by immersing Cu Pre-deposited steel into a mixture of 2.5 mol/L of NaOH and 0.1 mol/L of H_2O_2 solution at 60°C for 30 minutes.
- Stearic acid modification. Chemical modification using stearic acid was the last step in fabricating superhydrophobic Cu coating. The objective of this treatment was to create a low-energy layer on CuO-coated surface. Chemical modification was completed by immersing CuO-coated steel into stearic acid ethanol solution with various concentrations for 24 hours at room temperature. The stearic acid concentrations were varied ranging from 0.01, 0.05, 0.10, 0.15, to 0.20 mol/L.

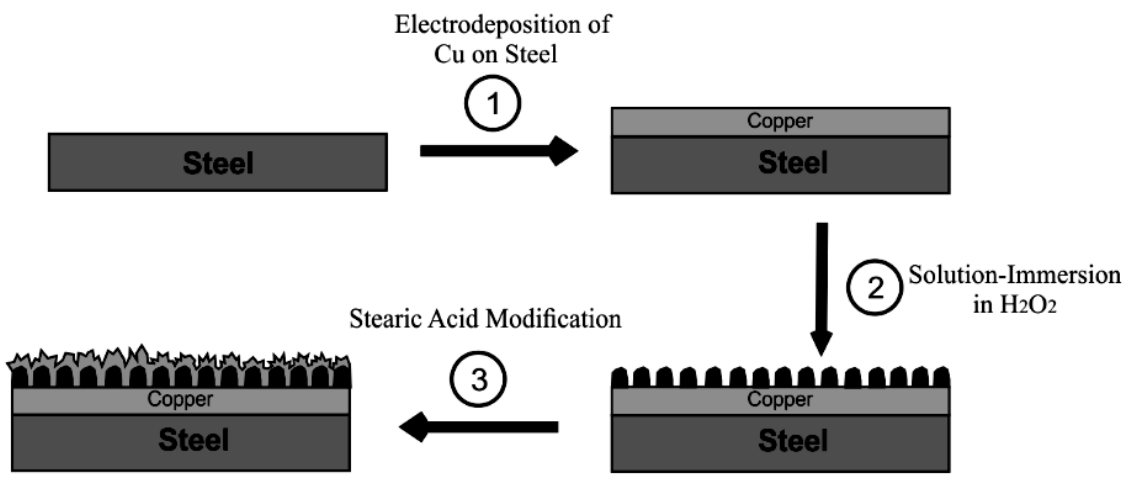

Fig. 1. Schematic diagram of the fabrication of superhydrophobic CuO coating.

Characterization procedures

The characterization tests performed in this work include measurement of contact angles, Scanning Electron Microscope (SEM) observation, and Energy Dispersive X-Ray Spectroscopy (EDS) measurements. The contact angle measurement includes static and dynamic contact angle measurements. These measurements were performed in order to characterize the wettability/superhydrophobicity of the coated surface under dynamic flow of water. The static contact angle was measured from ten different points on several specimens. The dynamic contact angle was obtained by investigating the effect of various treatments, which include Cu electrodeposition, Oxidation of Cu-coated steel, and stearic acid-modified CuO-coated steel, as well as the effect of stearic acid concentrations on dynamic contact angle. The analysis was performed using *ImageJ* DropSnake analysis (Stalder *et al.*, 2009).

The SEM and EDS measurements were conducted to characterize the surface morphology and chemical composition of the coated surface. A corrosion resistance test using a weight loss method was performed according to ASTM G1 to test the anti-corrosion property. Weight loss test method was used because it provided a facile yet reliable corrosion test result. The prepared superhydrophobic CuO samples were subjected to 5 wt% of NaCl solution by immersion for several days.

In addition, in order to test wettability of the solid surface, the specimen was subjected to immersion test in water as done and published by Hao Li et al. and Chao-Hua Xue et al. (Li *et al.*, 2016; Xue *et al.*, 2014). This test was not only to test the wettability of the surface but also to demonstrate the existence of air pocket in the microstructure interspace of superhydrophobic surface (Li *et al.*, 2016). The immersion test was a sequential process performed by dipping the specimen into distilled water for a couple of seconds and then the specimen was taken out afterward.

RESULTS AND DISCUSSION

Surface morphology and elemental analysis

Surface morphology of the prepared specimens obtained from SEM images and the chemical elements obtained from EDS analysis are shown in Figure 2. Based on EDS data in Fig. 2(a), it was known that bare steel specimen consisted of Fe, Mn, and Si, which are made up of 98.03 wt% of Fe, 1.57 wt% of Mn, and 0.40 wt% of Si.

The surface morphology and EDS spectrum of Cu-coated specimen are shown in Fig. 2(b). Based on the SEM image, the surface consisted of a nodular structure combined with a micro-sized flake-like structure. With this surface morphology, it was indicated that the bare steel specimen was completely coated with the copper element. The EDS spectrum also revealed that elements such as Fe, Mn, and Si did not exist on the Cu-coated surface. Cu-coated steel specimen was made up of 99.17 wt% Cu and a small amount of oxygen atom of 0.83 wt%. The absence of Fe element strongly indicated that the surface was fully covered with Cu. The small number of oxygen atoms was due to oxygen accumulation on the coating because of air agitation during electrodeposition.

The SEM image and EDS spectrum of Oxidized Cu-coated steel are presented in Fig. 2(c) above. It was observed that the oxidized Cu-coated specimen exhibited a remarkable change in morphology. According to SEM image of oxidized Cu-coated steel, the specimen surface was covered with micro-sized needle-like almost flower-like structure. It was indicated that the formation of $CuO/Cu(OH)_2$ hybrid layer contributed to the surface roughening. The EDS spectrum showed a significant rise in oxygen content. This was due to $CuO/Cu(OH)_2$ hybrid layers that existed on the surface during the oxidation process. It was found that Oxidized Cu-coated steel was composed of 70.22 wt% of Cu and 29.78 wt% of O elements.

The last specimen was stearic acid-modified CuO-coated steel. The SEM image of stearic acid modified CuO-coated steel is shown in Figure 2d. It was obvious that low-energy modification produced no significant changes in the morphological structure of the surface similar to reports in the literature (Hao *et al.*, 2016; Li and Yu, 2015). The surface of stearic acid modified CuO coating was covered by flower-like micro-sized, which was identical to the structure of CuO coating surface. It was a clear indication that stearic acid modification did not contribute to the surface morphology alteration. From the EDS spectrum, it showed that stearic acid modified surface consisted of 70.22 wt% of Cu and 29 wt% of O elements.

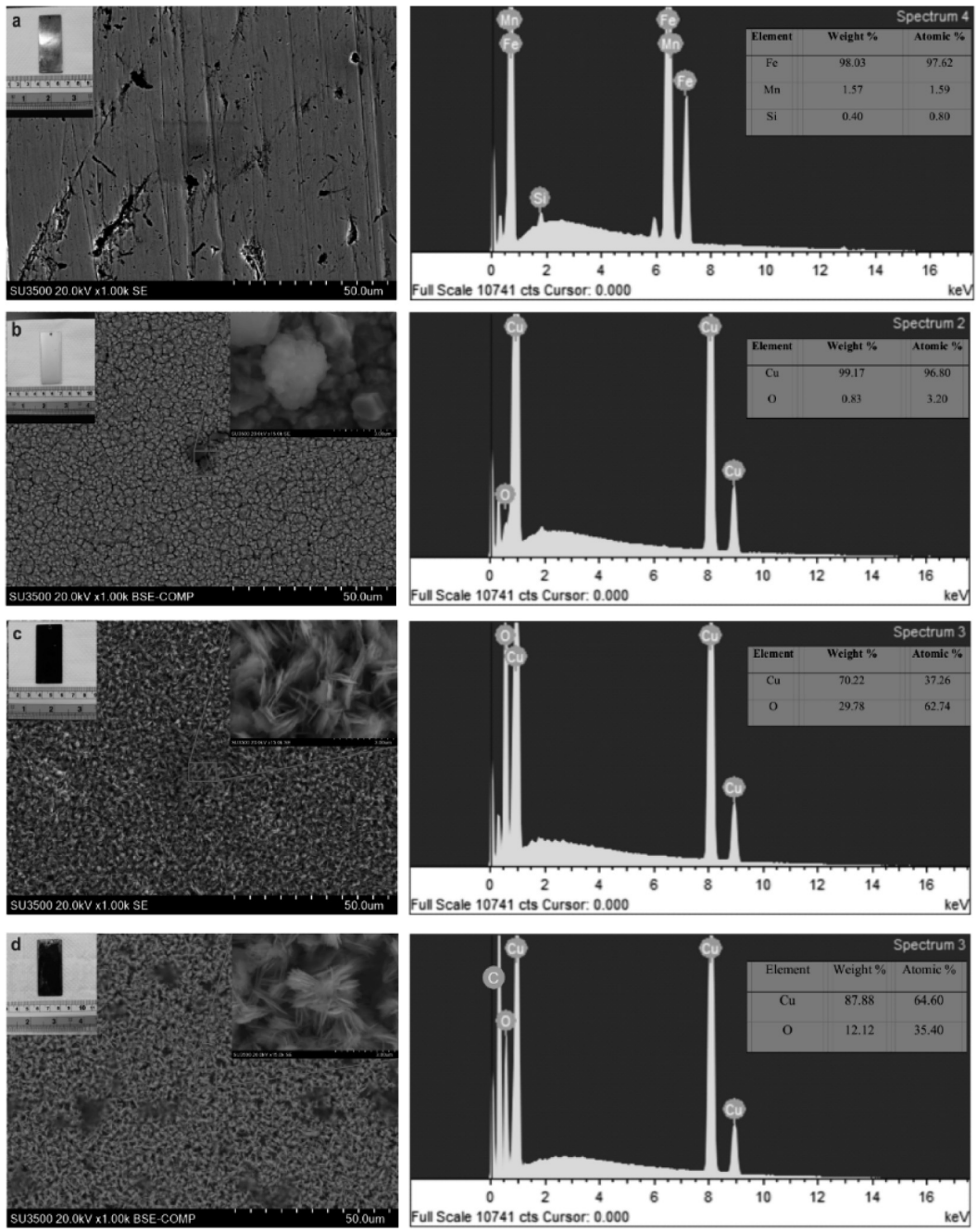

Fig. 2. SEM images and EDS spectra of: (a) Bare steel, (b) Cu-coated steel, (c) Oxidized Cu-coated steel, and (d) Stearic acid-modified Cu-coated steel.

The EDS spectrum in Fig. 2(d) revealed that the positions of the peaks of Cu and O element were also identical to the previous specimen, which were about 1, 8, 9, and 0.5 keV, respectively. However, a peak at around 0.27 keV indicated that carbon atoms were on the stearic acid modified surface and this is consistent with the ionization energy table value. Additionally, the stearic acid layer formation was proven by the reduction of oxygen atom content from 29.78 wt% on CuO-coated steel specimen to 12.12 wt% on the stearic acid modified specimen. It showed that CuO/$Cu(OH)_2$ hybrid layers were almost completely reacted with the carbonyl group of stearic acid.

Effect of various treatments on static contact angle

The static contact angles of specimens subjected to various processing treatments including bare/untreated steel, Cu-electrodeposition on steel, oxidation of Cu-coated steel, and stearic acid modification of CuO-coated steel are discussed. Static contact angles were measured at ten different points on the surface in order to make sure uniformity of the specimens. Table 1 shows the static contact angle for different treatments.

Table 1. Effect of processing condition on static contact angle.

Processing Conditions	**Static Contact Angle**
Bare Steel	73.5 ± 2.48°
Cu-Electrodeposited Steel	75.4 ± 1.81°
Oxidized Cu-Coated Steel	22.4 ± 2.50°
Oxidized Cu-Coated Steel + Stearic Acid	171.4 ± 1.56°

It was found that the contact angle of bare steel/untreated steel was 73.5° with the standard error of 2.48°. According to the result, the bare steel was hydrophilic. After Cu-electrodeposition treatment, the static contact angle had no significant change. Based on SEM images, Cu-coated surface exhibited a rise in surface roughness in compared to bare/untreated steel as shown in Figure 2.

The static contact angle was significantly reduced after oxidizing the Cu-coated surface. The static contact angle was reduced to 22.4° with the standard error of 2.5°. The significant decrease in contact angle was because of the presence of the hydroxyl group on the CuO layer that was very stable at temperature up to 400°C (Gurav *et al.*, 2014). The presence of the hydroxyl group was because CuO layer was fabricated by solution immersion at room temperature. The hydroxyl group has a polar behavior, so it is strongly attracted to water. Based on the static contact angle value, Oxidized Cu-coated steel had a hydrophilic surface.

On the contrary, after low-surface-energy treatment with stearic acid, the CuO-coated steel transformed from hydrophilic to superhydrophobic. The static contact angle was remarkably enhanced from 22.4 to 171.4° with the standard error being 2.50 and 1.56°, respectively. It was observed that the water droplet was rolled off as it touched the specimen surface. This superhydrophobicity was due to the non-polar tails pointing outward. As a result, non-polar tails repelled water so that water droplets easily rolled off the surface. The schematic illustration of the chemical reaction between stearic acid and the hydroxyl group on the CuO layer is shown in Figure 3.

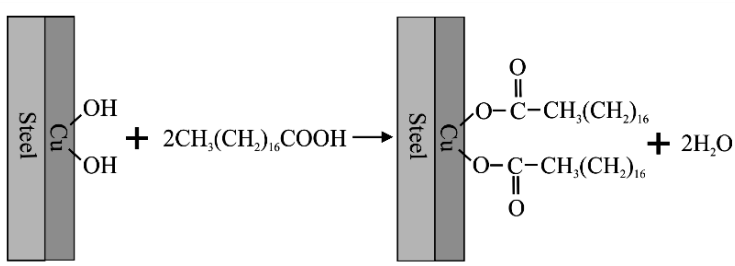

Fig. 3. Illustration of the reaction between stearic acid and hydroxyl group of CuO layer.

The reaction in Figure 3 can be expressed by the following reaction:

$$Cu(OH)_2 + 2CH_3(CH2)_{16}COOH \rightarrow CH_3(CH_2)_{16}COOCu + 2H_2O$$

Hydroxyl group in $Cu(OH)_2$ reacted with two molecules of $CH_3(CH_2)_{16}COOH$ by the chelating reaction. OH^- ions in copper (II) hydroxide reacted with H^+ ions in stearic acid molecules. Furthermore, carbonyl group, $CH_3(CH_2)_{16}COO$ in stearic acid, reacted with CuO layer to form $CH_3(CH_2)_{16}COOCu$ with CH_3 group facing out of the surface. The effect of the addition of stearic acid in every processing condition is also discussed.

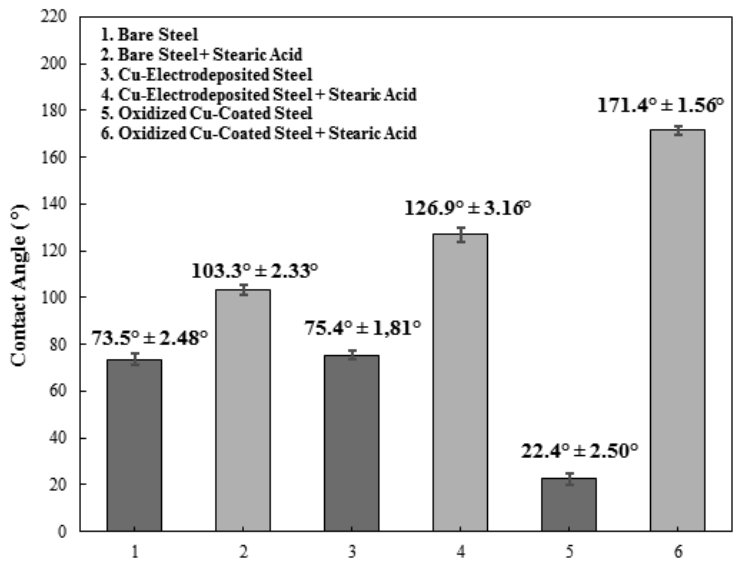

Fig. 4. Effect of stearic acid addition to each processing condition.

The following discussions are aimed to observe the changes of contact angles when stearic acid was added to each of the initial processing conditions. The comparison of contact angle values for different treatments can be seen in Figure 4. It was found that the addition of stearic acid to each initial processing condition enhanced hydrophobicity. As shown in the bar chart in Figure 4, the static contact angle of bare steel after stearic modification was enhanced to 103.3° with standard error of 2.33°. It showed that the contact angle of bare steel treated with stearic acid increased by approximately 30° compared to untreated bare steel. In addition, there was an increase in the contact angle of Cu-coated steel after stearic acid modification from 75.4 to 126.9°. This suggested that the formation of rough structures on Cu-coated steel in combination with stearic acid contributed to contact angle enhancement, which satisfied the Wenzel's model. According to Wenzel's model, the water droplet will penetrate into a surface through rough structure interspace.

There was also a notable rise in contact angle after stearic acid modification on Oxidized Cu-coated/CuO-coated steel. It was observed that the static contact angle of stearic acid modified CuO layer increased to 171.4 from 22.4°. This showed that the addition of stearic acid to the flower-like CuO layer enhanced the superhydrophobicity property of the surface. This finding showed that the combination of flower-like/rough structure with a low-surface-energy modifier such as stearic acid was the main factor to achieve superhydrophobicity. With a contact angle of 171.4°, it was suggested that the wetting behavior satisfied Cassie-Baxter's model. It happened when the water droplets were suspended on the flower-like CuO structure due to the formation of air pocket in the structure, as illustrated in Figure 5.

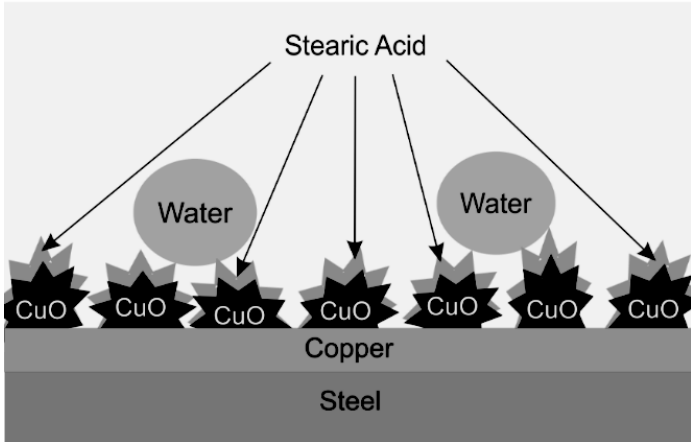

Fig. 5. Wetting behavior of superhydrophobic surface.

Effect of stearic acid concentrations on static contact angle

The wettability of the surface after modification using stearic acid was investigated. The wettability or hydrophobicity of stearic-modified CuO layer on the substrate was analyzed by both static and dynamic contact angle measurements. Static contact angle measurement was performed by dropping about 10 μL of distilled water onto the substrate's surface, which had been modified with various concentrations of stearic acid. The measurements were performed at 10 different points on the surface at room temperature (~23°C). The values of the static contact angle on stearic modified CuO surface are provided in Table 2.

Table 2. Static contact angle values of different stearic acid concentrations.

Stearic Acid Concentration (mol/L)	Static Contact Angle
0.01	156 ± 2.19°
0.05	171.4 ± 1.56°
0.10	158 ± 2.41°
0.15	97.5 ± 2.72°
0.20	104 ± 4.48°

The static contact angle at 0.01 mol/L stearic acid was about 156° with standard error from the measurement of about 2.19°. After adding stearic concentration to 0.05 mol/L, the static water contact angle was significantly enhanced to 171.4° with standard error of 1.56°. This implied that the stearic acid modified CuO layer was superhydrophobic because the water contact angle was above 150°. The superhydrophobicity was due to the stearic acid molecule reaction with hydroxyl group on CuO layer forming copper stearate molecule with its non-polar chain exposed to the substrate surface.

By increasing stearic concentration from 0.01 to 0.05 mol/L, the static water contact angle also increased. This happened due to change in surface roughness and addition of non-polar stearate molecule that enhanced superhydrophobicity. Furthermore, increasing stearic acid concentration to 0.10, 0.15, and 0.20 mol/L resulted in a static contact angle reduction to 158, 97.5, and 104° with the standard error of 2.41, 2.72, and 4.48°, respectively. This phenomenon suggested that increasing stearic concentration will lead to stearate over-coverage that consequently reduces the roughness of the surface. Importantly, from the data in Table 2, it could be seen clearly that the optimum stearic concentration with the highest contact angle was 0.05 mol/L.

Dynamic contact angle results

In this section, the discussion is aimed to elaborate on the correlation between sliding angle and static contact angle at various concentrations of stearic acid. According to Figure 6, the sliding angle had a negative correlation with static contact angle. It was found that the sliding angle was reduced as the static contact angle increased. From our measurements, the sliding angles were 11.9 ± 1.14°, 7.2 ± 0.43°, 14.9 ± 1.59°, 40.6 ± 2.18°, and 41.1 ± 1.68°, for stearic acid concentration of 0.01, 0.05, 0.10, 0.15, and 0.20 mol/L, respectively. The results showed that 0.05 mol/L with sliding contact angle of 7.2 ± 0.43° was the most optimum result. It was concluded that the superhydrophobic CuO coating prepared in this experiment had an extremely high contact angle and low sliding angle. This finding was consistent with the one that had been obtained by a previous study (Gurav *et al.*, 2014).

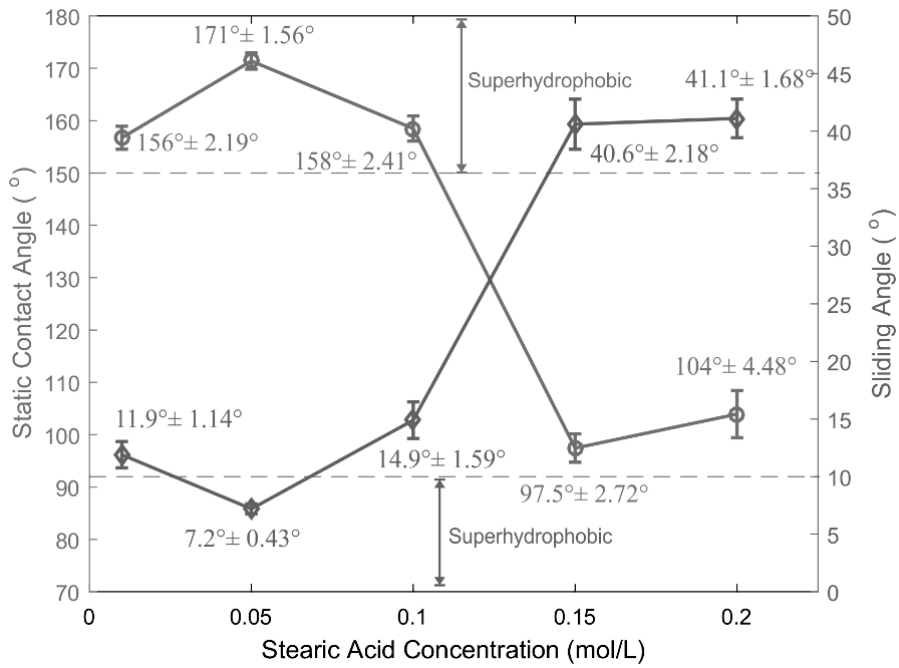

Fig. 6. Correlation between sliding angle and static contact angle at various stearic acid concentrations.

Corrosion test results

The relationship between stearic acid concentration and the corrosion rate of stearic-acid-modified CuO-coated steel is shown in Figure 7. It was found that the increase of stearic acid concentration also led to corrosion rate elevation for 7 and 10 days of immersion in 5 wt% of NaCl solution. The corrosion rate of around 0.05 mm/year was noted when the sample was treated with 0.01 mol/L of stearic acid. As stearic acid raised to 0.15 mol/L, the identical trends were also observed. When the concentration was raised to 0.2 mol/L, the corrosion rate also increased gradually with small fluctuation to 0.18 and 0.15 mm/year for 7 and 10 days of immersion, respectively. This finding was consistent with the effect of stearic acid on the static contact angle. Interestingly, the corrosion rate at 0.15 mol/L indicated identical values for 7 and 10 days of immersion in the NaCl solution. It is because of at 0.15 mol/L that there was a change of state from hydrophilic state to hydrophobic surface state (contact angle of around 90°). It was also described further in the graph of contact angle where there was an inflection point that occurred at 0.15 mol/L and this inflection point suggested surface behavior changes similar to the corrosion test results.

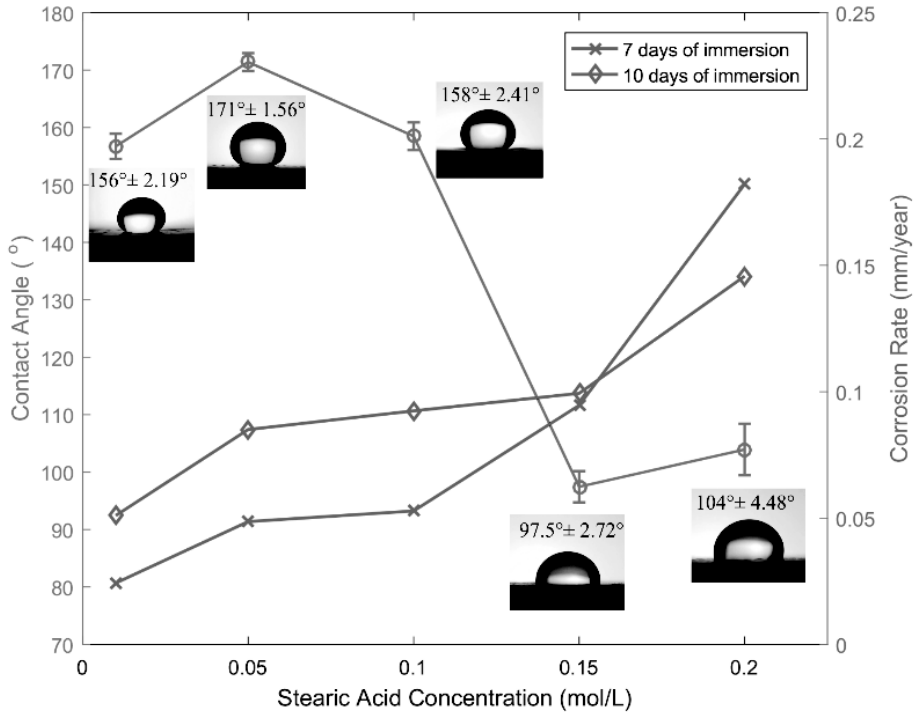

Fig. 7. Correlation between corrosion rate and static contact angle at various stearic acid concentrations.

The experimental results of corrosion rate also showed that there was a negative correlation between contact angle values and corrosion rate. As the surface lost its hydrophobicity indicated by declining in contact angle values, the corrosion rate would increase accordingly. In other words, hydrophobicity possesses anti-corrosion property according to this experiment. The anti-corrosion property worked by inhibiting the corrosion agents to penetrate the surface of the structure. Furthermore, the corrosion inhibition efficiency data is shown in Figure 8. The corrosion inhibition efficiency was calculated by this following equation (1) (Lestari and Priyotomo, 2018):

$$\%I_{eff} = \frac{Cr - Cr_{inh}}{Cr} \times 100\% \quad (1)$$

where Cr is the corrosion rate of the specimen without inhibitor and Cr_{inh} is the corrosion rate of the inhibited specimen. It was found that corrosion inhibition efficiency diminished as stearic acid concentration increased. This was consistent with corrosion rate data in Figure 7. Initially, corrosion inhibition efficiency was above 90% for the stearic acid concentration of 0.01 mol/L. It then gradually reduced as stearic acid concentration was added to 0.2 mol/L. However, the efficiency was still above 70% for the stearic acid concentration of 0.2 mol/L. It showed that stearic acid modification contributed to anti-corrosion property of the solid surface.

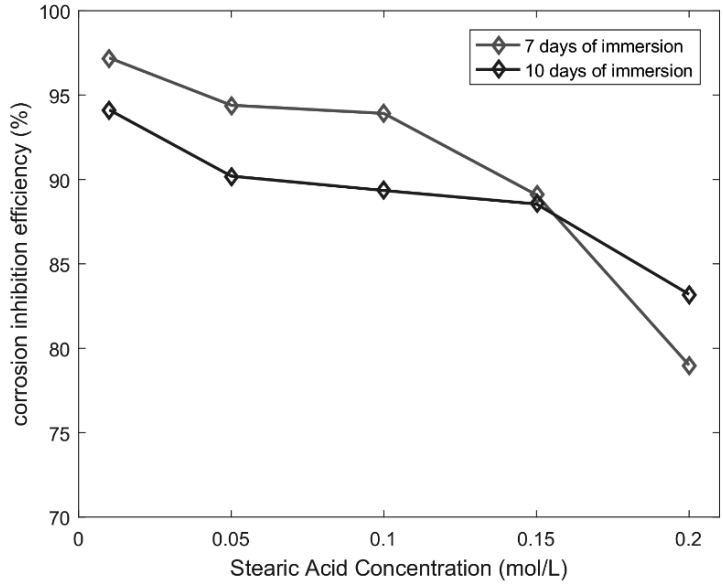

Fig. 8. Corrosion inhibition efficiency of various stearic acid concentration.

Wettability test results

Figure 9 demonstrates the wettability test of superhydrophobic CuO coating on steel specimen. During immersion, the submerged part of the sample exhibited bright silver-like plastron layer (Li *et al.*, 2016; Xue *et al.*, 2014). This bright layer was due to total internal reflection of light at air pocket on the sample surface. It showed that the superhydrophobic surface contained air pockets, which were trapped between micro-structures of the surface (Xue *et al.*, 2014). According to the observation conducted by naked eye, the specimen showed no water attached to the surface after the immersion test. It was completely dry as before immersion.

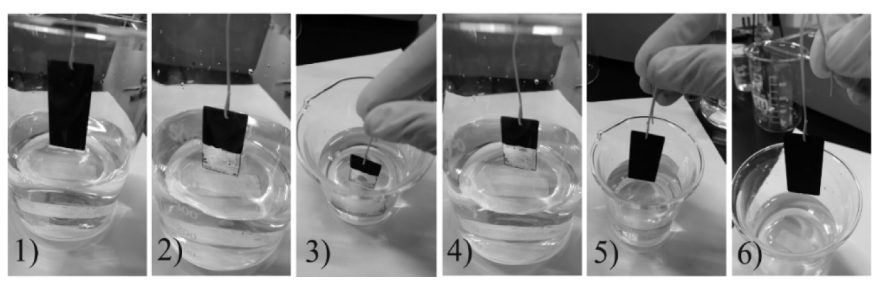

Fig. 9. Immersion test of Superhydrophobic CuO coating in distilled water.

This result showed that the air pocket could effectively prevent the water from penetrating into the surface. It had been found that at atmospheric pressure the water droplet must exceed the intrusion pressure (ΔP) in order to penetrate into the coating (Li *et al.*, 2016). It is defined as the amount of pressure that a coating can withstand before the water can penetrate into it. The intrusion pressure is expressed by the following equation (2):

$$\Delta P = \frac{-l\gamma cos\theta}{A} \tag{2}$$

where l and A are the perimeter and area of the interspace between microstructure, respectively. γ is the water surface tension and θ is the water contact angle. As the surface was superhydrophobic (contact angle > 150°), the

value of ΔP was bigger 0. It was implied that the coating had relatively higher pressure than the water droplets. It was proven that the surface was impenetrable by water. These results also showed that there was a positive indication that superhydrophobic CuO coating could be used for self-cleaning application. Moreover, with such distinctive properties, superhydrophobic CuO coating could be used to study wave propagation in fluid-structure interaction, which had been reported in the literature (Kojima *et al.*, 2017).

CONCLUSION

Through a series of treatments including Cu electrodeposition, alkali solution immersion, and stearic acid modification, a superhydrophobic CuO coating on steel substrate had been successfully fabricated. The static contact and sliding angles were found to be 171.4 ± 1.56° and 7.2 ± 0.43°, respectively, which indicated the superhydrophobicity property. Moreover, superhydrophobic CuO coating prepared in this study showed a flower-like microstructure. In addition, it also exhibited an anti-corrosion property. It was found that the superhydrophobic CuO coating had a corrosion inhibition efficiency of more than 70%.

ACKNOWLEDGMENT

This work was supported by CRCS (Center of Research and Community Service), Sampoerna University. SEM and EDS were performed at Research Center for Physics, Indonesian Institute of Sciences.

REFERENCES

Asmara, Y. & Kurniawan, T. 2018. Corrosion prediction for corrosion rate of carbon steel in oil and gas environment: A review. Indonesian Journal of Science and Technology **3**(1): 64-74.

Brassard, J.D., Sarkar, D.K., Perron, J., Audibert-Hayet, A. & Melot, D. 2015. Nano-micro structured superhydrophobic zinc coating on steel for prevention of corrosion and ice adhesion. Journal of Colloid and Interface Science: 240-247.

Feng, Y., Chen, S. & Cheng, Y.F. 2018. Stearic acid modified zinc nano-coatings with superhydrophobicity and enhanced antifouling performance Surface & Coating Technology **340**: 55-65.

Ganapathy, V., Kurniawan, T., Ayu, H.M., Asmara, Y.P., Daud, R., Prastomo, N. & Nandiyanto, A.B.D. 2018. Aluminum alloy AA2024 coated with ZrO2 using a sol-gel-assisted dip-coating technique and its corrosion performance. Journal of Engineering Science and Technology **13**(6): 1713-1721.

Gurav, A.B., Latthe, S.S., Vhatkar, R.S., Lee, J.-G., Kim, D.-Y., Park, J.-J. & Yoon, S.S. 2014. Superhydrophobic surface decorated with vertical ZnO nanorods modified by stearic acid. Ceramics International **40**: 7151-7160.

Hao, L., Sirong, Y. & Xiangxiang, H. 2015. Preparation of a biomimetic superhydrophobic ZnO coating on an X90 pipeline steel surface. New Journal of Chemistry **39**(6): 4860-4868.

Hao, L., Sirong, Y. & Xiangxiang, H. 2016. Fabrication of CuO hierarchiacal flower-like structures with biomimetic superamphiphobic, self-cleaning and corrosion resistance properties. Chemical Engineering Journal: 1443-1454.

Kojima, T., Inaba, K., Takahashi, K., Triawan, F. & Kishimoto, K. 2017. Dynamics of Wave Propagation Across Solid-Fluid Movable Interface in Fluid-Structure Interaction. J. Pressure Vessel Technol **139**(3).

Kong, L.H., Chen, X.H., Yu, L.G., Wu, Z.S. & Zhang, P.Y. 2015. Superhydrophobic Cuprous Oxide Nanostructures on Phosphor-Copper Meshes and Their Oil–Water Separation and Oil Spill Cleanup. ACS Applied Materials & Interfaces: 2616-2625.

Kurniawan, T., Fauzi, F.A.B. & Asmara, Y.P. 2016. High-temperature oxidation of Fe-Cr steels in steam condition–A review. Indonesian Journal of Science and Technology **1**(1): 107-114.

Lestari, Y. & Priyotomo, G. 2018. Corrosion resistance of API 5L grade B steel with taro leaf (Colocasia esculenta) addition as corrosion inhibitor in HCl 0.1 M. AIP Conference Proceeding. American Institute of Physics.

Li, H. & Yu, S. 2015. Facile fabrication of micro-nano-rod structures for inducing a superamphiphobic property on steel surface. Applied Physics A **122**(1).

Li, H., Yu, S., Han, X. & Zhao, Y. 2016. A stable hierarchical superhydrophobic coating on pipeline steel surface with self-cleaning, anticorrosion, and anti-scaling properties. Colloids and Surfaces A: Physicochemical and Engineering Aspects: 43-52.

Li, H. & Yu, S. 2016. A stable superamphiphobic Zn coating with self-cleaning property on steel surface fabricated via a deposition method. Journal of the Taiwan Institute of Chemical Engineers: 1-10.

Li, H. & Yu, S. 2017. Fabrication and theoretical explanation of the superhydrophobic CueZn coating with dandelion-like CuO microstructure. Journal of Alloys and Compounds: 195-205.

Stalder, A.F., Kulik, G., Sage, D., Barbieri, L. & Hoffmann, P. 2009. A snake-based approach to accurate determination of both contact points and contact angles. Colloids and Surfaces A: 92-103.

Subramanyam, S.B., Kondrashov, V., Ruhe, J. & Varanasi, K.K. 2016. Low Ice Adhesion on Nano-Textured Superhydrophobic Surfaces under Supersaturated Conditions. Applied Materials & Interfaces: 12583-12587.

Triawan, F., Nandiyanto, A.B.D., Abdullah, A.G. & Aziz, M. 2018. Plasma nitriding time on the hardness and crystal structure/phase of SUS403 and SCS6 martensitic stainless steels: An analytical study. Journal of Engineering Science and Technology **13**(8): 2369-2378.

Trisnanto, S.R., Sunnardianto, G.K. & Setiawan, I. 2018. Fabrication of superhydrophobic CuO coating on steel by electrodeposition modified with stearic acid. 4th International Conference on Computing Engineering and Design. Bangkok: IEEE.

Vazirinasab, E., Jafari, R. & Momen, G. 2018. Application of superhydrophobic coatings as a corrosion barrier: A review. Surface & Coatings Technology **341**: 40-56.

Wen, Q., Guo, F., Peng, Y. & Guo, Z. 2018. Simple fabrication of superamphiphobic copper surfaces with multilevel structures. Colloid and Surfaces A **539**: 11-17.

Whelan, C.M., Kinsella, M., Ho, H.M. & Maex, K. 2004. Corrosion inhibition by thiol-derived SAMs for enhanced wire bonding on Cu surfaces. Journal of The Electrochemical Society **151**(2): B33-B38.

Xue, C.-H., Li, Y.-R., Zhang, P., Ma, J.-Z. & Jia, S.-T. 2014. Washable and Wear-Resistant Superhydrophobic Surfaces with Self-Cleaning Property by Chemical Etching of Fibers and Hydrophobization. Applied Materials & Interfaces: 10153-10161.

Zhang, H., Yin, L., Shi, S., Liu, X., Wang, Y. & Wang, F. 2015. Facile and fast fabrication method for mechanically robust superhydrophobic surface on aluminum foil. Microelectronic Engineering **141**: 238-242.

Zhang, J., Liu, Z., Liu, J., E, L. & Liu, Z. 2016. Effects of seed layers on controlling of the morphology of ZnO nanostructures and superhydrophobicity of ZnO nanostructure/stearic acid composite films. Materials Chemistry and Physics **183**: 306-314.

Zhang, Y., Ge, D. & Yang, S. 2014. Spray-coating of superhydrophobic aluminum alloys with enhanced mechanical robustness. Journal of Colloid and Interface Science **423**: 101-107.